TDOT Department of Transportation

U.S. Department of Transportation
Federal Highway Administration

Load Rating of Girder-Stringer-Floorbeam Bridges

Research Final Report from Tennessee Tech University | R. Craig Henderson, Tim Huff, Matt Yarnold | January 19, 2023

Sponsored by Tennessee Department of Transportation Long Range Planning Research Office & Federal Highway Administration

DISCLAIMER

This research was funded through the State Planning and Research (SPR) Program by the Tennessee Department of Transportation and the Federal Highway Administration under ***RES2022-02, Research Project Title: Load Rating of Girder-Stringer-Floorbeam Bridges.***

Technical Report Documentation Page

1. Report No. RES2022-02	2. Government Accession No.	3. Recipient's Catalog No.
4. Title and Subtitle *Load Rating of Girder-Stringer-Floorbeam Bridges*		5. Report Date January 31, 2023 6. Performing Organization Code
7. Author(s) R. Craig Henderson, Ph.D., P.E. Tim Huff, Ph.D., P.E. Matt Yarnold, Ph.D., P.E.		8. Performing Organization Report No.
9. Performing Organization Name and Address Tennessee Technological University P.O. Box 5015 Cookeville, TN 38505		10. Work Unit No. (TRAIS) 11. Contract or Grant No. RES2022-02
12. Sponsoring Agency Name and Address Tennessee Department of Transportation 505 Deaderick Street, Suite 900 Nashville, TN 37243		13. Type of Report and Period Covered 14. Sponsoring Agency Code
15. Supplementary Notes Conducted in cooperation with the U.S. Department of Transportation, Federal Highway Administration		

16. Abstract

The research described herein investigated the behavior and capacity of girder-string-floorbeam bridges by:

- Conducting a literature review of the current state-of-practice and emerging research regarding the capacity and behavior of girder-stringer-floorbeam bridges;
- Experimentally measuring strain at various locations and identifying characteristic behavior in the stringers and girders of the Billy Nance Memorial Highway Bridge under live load; and
- Conducting line girder analysis of continuous stringer spans using SIMON software and identifying potential sources of refined load ratings.

Upon evaluation of the diagnostic load testing results, it can be inferred that the stringers in the girder-stringer-floorbeam bridge, SR-114 over the Tennessee River, have a higher load rating than initially anticipated. This is due, in part, to the fact that the stringers act semi-compositely with the concrete bridge deck (proven by the strain profile at the member cross-sections) which allows for a higher capacity in the stringers. In addition, the live load demands on the stringers were observed to be less than anticipated. Other sources of undue conservatism in typical stringer rating calculations were identified as well.

17. Key Words **GIRDER, STRINGER, FLOORBEAM, BRIDGE, TESTING, COMPOSITE ACTION**	18. Distribution Statement		
19. Security Classif. (of this report) Unclassified	20. Security Classif. (of this page) Unclassified	21. No. of Pages xxx	22. Price

Acknowledgements

The authors would like to thank our TDOT technical contacts, particularly Rebecca Hayworth, for their leadership and coordination of this project. The close partnership between the TDOT technical team and the TTU/Auburn researchers was much appreciated.

The authors would also like to thank TDOT logistical and traffic control personnel (particularly Jennifer Blankenship, Jason Ellison, and Ronnie Moore). Great job! Thanks for keeping us all safe.

Executive Summary

GOALS AND PURPOSE: There are 31 bridges in Tennessee with superstructure systems consisting of steel girders, floor beams, and stringers. The results of Tennessee Department of Transportation (TDOT) load rating calculations, mandated by Federal Highway Administration (FHWA), have shown low capacity for some of these bridges (using various methods and software), particularly in the stringers. As a result, an experimental and analytical research program was initiated, and it focused on a representative bridge in Hardin County: Billy Nance Memorial Highway Bridge.

The research described herein investigated the behavior and capacity of girder-string-floorbeam bridges by:

- Conducting a literature review of the current state-of-practice and emerging research regarding the capacity and behavior of girder-stringer-floorbeam bridges.
- Experimentally measuring strain at various locations and identifying characteristic behavior in the stringers and girders of a representative bridge under live load; and
- Conducting line girder analysis of continuous stringer spans using SIMON software and identifying potential sources of refined load ratings.

LITERATURE REVIEW: Few published articles were found that had substantial bearing on the refinement of ratings for stringers. However, one exception is an article by Kuruppuarachchi (2021) who conducted research on the flexural capacity of continuous stringers as affected by the moment gradient factor, Cb. The recommended equations produce Cb values that are similar to finite element analysis and lab testing data and result in substantial increases in the load ratings of continuous stringers. Increased Cb values are discussed along with seven additional refinement options.

EXPERIMENTAL TEST PROCESS: The steel portion of the representative test bridge (SR-114) consists of three girders supported by concrete piers and connected by cross-frames at 25 ft spacing.

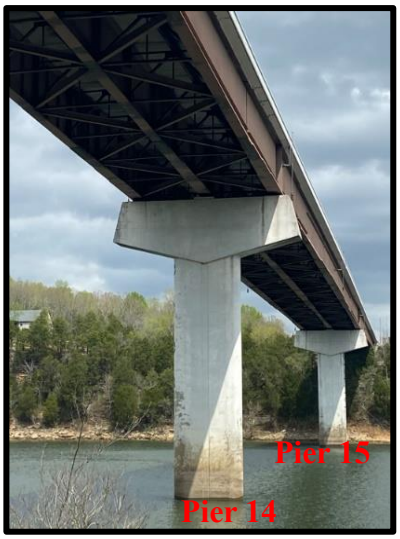

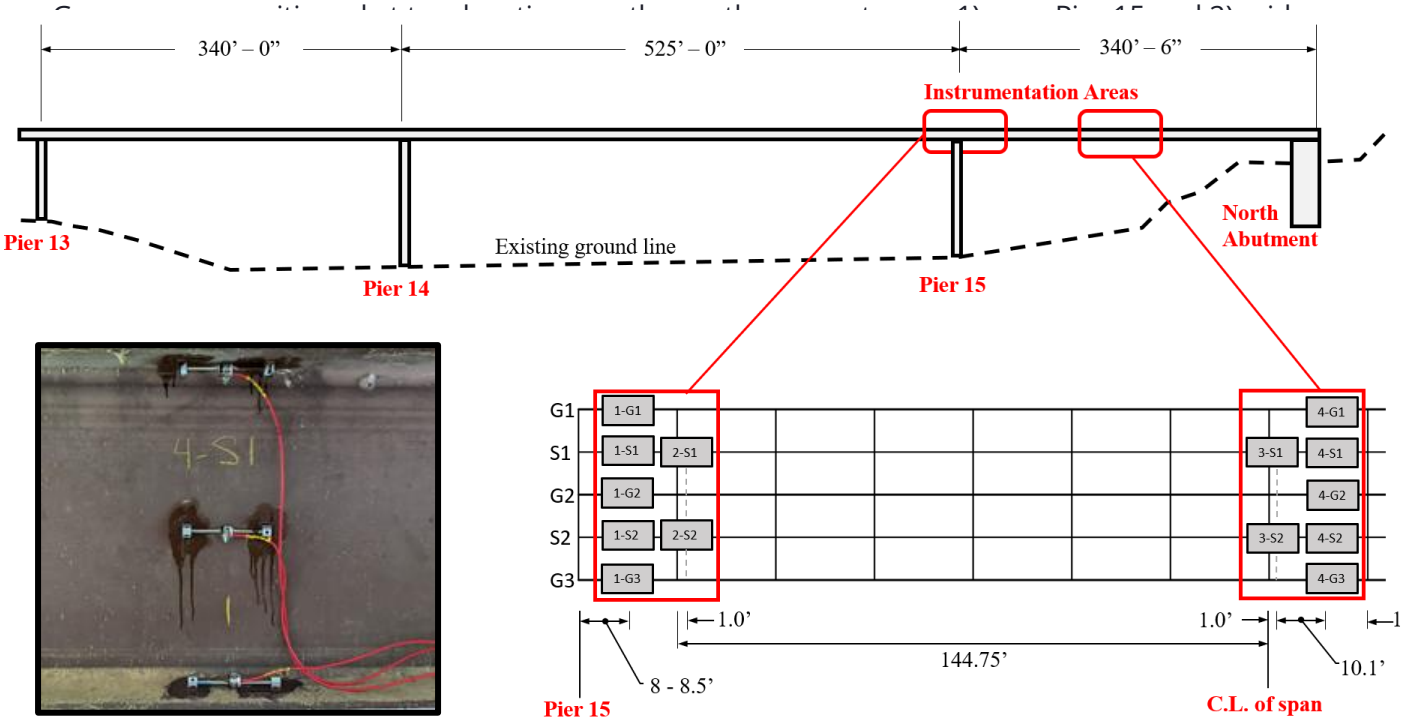

Strain gauges and the associated data acquisition equipment were installed under the bridge using a reach-all vehicle. Gauges were placed on the top and bottom flanges as well as the center of the web for both stringers and girders to capture the flexural strain profile throughout the cross-section.

Standard five-axle TDOT dump trucks were used for the load testing. The total truck weight was recorded and then verified using scales placed under each of the truck wheels. The two middle axles were raised and disregarded during the weighing and load testing.

Four load tests (i.e., A, B, C, and D) were conducted with different truck locations to produce worst-case negative and positive moments on the stringers. For each load test, the trucks were positioned at Pier 15 and moved slowly (i.e., approximately 10 miles per hour) across the instrumented span (i.e., the end-span). For Load Cases A, C, and D, the trucks moved continuously until exiting the bridge. For Load Case B, the trucks stopped at mid-span between

Piers 14 and 15 and between Pier 15 and the North abutment to induce maximum negative moment in the stringers and girders at Pier 15.

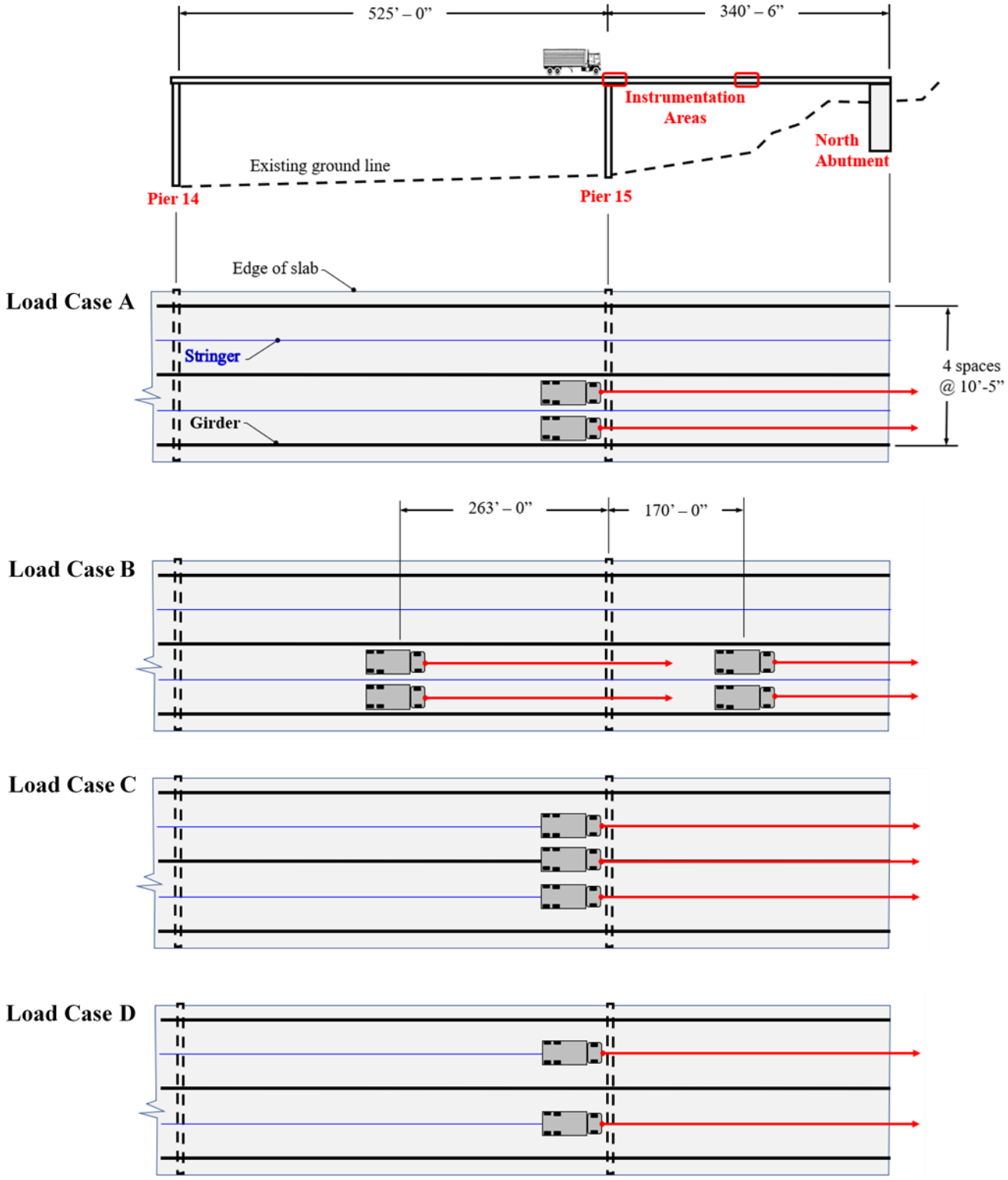

All the collected strain data for each gauge at each location was stored in a comma-delimited format and imported into MATLAB for processing and interpretation. The worst-case strains (i.e., worst-case microstrain values for the top and bottom flange and the web) were plotted at each location on the stringers and girders (e.g., 1-G1, 1-S1, etc.) Maximum and minimum strain readings for each gauge were determined and used in the analytical evaluation.

1-G1		Micro Strain	
		Minimum	Maximum
DAQ 1 (BDI)			
1	1-G1-TF	-0.4	10.3
2	1-G1-W	-3.6	1.5
3	1-G1-BF	-12.1	6.6

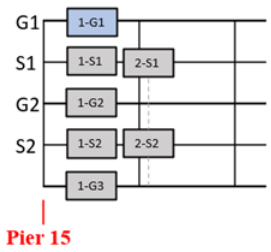

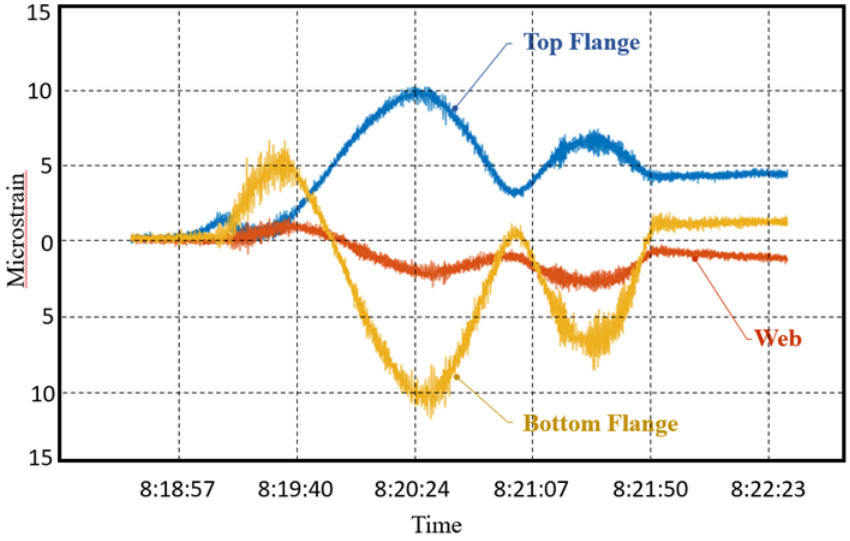

ANALYTICAL EVALUATION: The following eight areas were identified and investigated as potential sources of refined load ratings for stringers in girder-stringer-floorbeam bridges.

1. Live Load Distribution Factors;
2. Moment Gradient Factor (C_b);
3. Critical Stress (F_{cr}) Calculation;
4. Appendix A6 vs. Chapter 6 Provisions;
5. Diagnostic Load Testing;
6. Low Traffic Volumes;
7. Condition and System Factors; and
8. Wearing Surface Elimination

Appendix A6, in the American Association of State Highway and Transportation Officials (AASHTO) Specification, is permitted for members with compact webs and permits plastification of the web. For members which have compact webs and satisfy all requirements in Appendix 6, flexural resistance may be based on the plastic moment, while provisions in Chapter 6 limit flexural resistance to the yield moment.

It has been established in previous studies that the 'default' moment gradient factor, C_b, is overly conservative for members such as stringers in girder-stringer-floorbeam bridges. More refined and accurate C_b-factors were taken from the literature and from the American Institute of Steel Construction (AISC) 360-16 and used in this study.

Standard critical stress calculations from Chapter 6 of the AASHTO Specifications ignore a term that is included in Appendix 6. The calculation in Chapter 6 is likely appropriately neglected for typical, welded plate girder members found in bridges. However, for rolled shapes used in

stringers, the term is significant and should be included. For the stringers studied in this project, the inclusion of the term resulted in a 30% increase in critical stress.

Theoretical strains for this study were computed based on lever rule live load distribution factors. Measured strains from diagnostic load testing were found to be significantly less than lever rule-based theoretical strains.

Striped lane distribution factors are permitted by the AASHTO Manual for Bridge Evaluation (MBE). For the SR-114 bridge load tested, a single-lane distribution factor could be justified, given that each side of the bridge centerline consists of a single striped lane with a single stringer.

For bridges with Average Daily Truck Traffic (ADTT) of less than 5000 trucks per day, the AASHTO MBE permits the standard live load factor of 1.45 to be reduced to a value as low as 1.30.

Key Findings

- Standard, default C_b-factors in modern software are overly conservative for stringers in girder-stringer-floorbeam bridges.
- Application of the more exact expression for critical stress found in Appendix A6 of the AASHTO Specifications is appropriate for stringers and results in significantly increased flexural resistance.
- Application of additional Appendix A6 provisions, when allowed, permits the plastic flexural resistance to be used. Modern software typically limits flexural resistance to the first yield.
- Measured strains in stringers are typically significantly less than theoretical values obtained using lever rule live load distribution. The controlling K-factor (a direct amplification of the rating) for the load-tested bridge was found to be 1.68.

Key Recommendations

- Use refined C_b-factors.
- Use lever rule live load distribution.
- Apply Appendix A6 provisions when applicable. The anticipation is that most, if not all, stringers in TDOT bridges will have compact webs and satisfy the conditions required in Appendix A6.
- Eliminate wearing surface loads when no wearing surface is present.

In cases where rating deficiencies are still indicated after applying the above four items, consider each of the following in succession:

- For low-volume roads (ADTT less than 5000 trucks per day), reduce load factors in accordance with MBE Table 6A.4.4.2.3b-1.
- Perform diagnostic load testing to establish an appropriate K-factor for rating refinement.
- Consider the refined condition and system factors in accordance with National Cooperative Highway Research Program (NCHRP) Report 406.

Future research may include the load testing of additional bridges to establish appropriate K-factors for more accurate rating of stringers in girder-stringer-floorbeam bridges.

Table of Contents

DISCLAIMER i
Technical Report Documentation Page ii
Acknowledgement iii
Executive Summary iv
Key Findings viii
Key Recommendations viii
List of Tables xi
List of Figures xii
Glossary of Key Terms and Acronyms xiii
Chapter 1 Goals and Purpose 1
Chapter 2 Literature Review 2
2.1 Evaluation of a Noncomposite Steel Girder Bridge through Live-Load Field Testing 2
2.2 Instrumentation During Live Load Testing and Load Rating of Five Slab-on-Girder Bridges 3
2.3 Lateral Torsional Buckling Resistance of Continuous Steel Stringers in Existing Bridges 4
2.4 Relevance of Reviewed Articles 5
Chapter 3 Experimental Test Process 6
3.1 Instrumentation 6
3.1.1 General Strain Gauge Locations 6
3.1.2 Specific Strain Gauge Placement on Stringers and Girders 8
3.1.3 Strain Gauge Placement Method and Connection to the Data Acquisition System 9
3.2 Testing 10
3.2.1 Truck Dimensions and Axle Weights 10
3.2.2 Truck Load Placement and Sequence 12
3.2.3 Bridge Loading 14
3.3Data Processing and Test Results 14
3.3.1 Introduction 14
3.3.2 Load Test Strains associated with MBE K-Factor 15
Chapter 4 Analytical Evaluation 18
4.1 Live Load Distribution Factors for Stringers 18
4.2 Lateral-Torsional Buckling Modification Factor (C_b) 19
4.3 Critical Stress (F_{cr}) Calculation 20
4.4 Appendix A6 Provisions vs. Chapter 6 Provisions 21

4.5 Diagnostic Load Testing 23
4.6 Low Traffic Volumes 24
4.7 Condition and System Factors 25
4.8 Elimination of Wearing Surface Loading Where Appropriate 27
Chapter 5 Results and Discussion 28
Chapter 6 Conclusion 32
References 33

List of Tables

Table 3-1. Gauge Location and Behavior 7
Table 3-2. Truck Axle Weights 11
Table 4-1. Values for K_b in the MBE 24
Table 4-2. MBE-Specified Load Factors 25
Table 4-3. NCHRP Report 406 System Factors 26

List of Figures

Figure 3-1. General Strain Gauge Placement 6
Figure 3-2. Bridge Member Configuration 6
Figure 3-3. Global and Local Bending of Stringers 7
Figure 3-4. Reach-all 8
Figure 3-5. Strain Gauge Placement on Typical Stringer 8
Figure 3-6. Shear Strain Measurement 9
Figure 3-7. Strain Gauge Placement 10
Figure 3-8. Cabling and DAQ Connection 10
Figure 3-9. TDOT Five Axle Dump Truck 11
Figure 3-10. Truck Dimensions 11
Figure 3-11. Load Test A 12
Figure 3-12. Load Test B 13
Figure 3-13. Load Test C 13
Figure 3-14. Load Test D 14
Figure 3-15. Strain and K-factor Calculation for Load Test A 15
Figure 3-16. Strain and K-factor Calculation for Load Test B 16
Figure 3-17. Strain and K-factor Calculation for Load Test C 17
Figure 3-18. Strain and K-factor Calculation for Load Test D 17
Figure 4-1. Stringer Boundary Conditions (AISC) 20
Figure 5-1. Standard Rating - SR-114 Stringers 30
Figure 5-2. Refined Rating - SR-114 Stringers 31

Glossary of Key Terms and Acronyms

AASHTO	American Association of State Highway and Transportation Officials
ADTT	Average Daily Truck Traffic
AISC	American Institute of Steel Construction
BDI	Bridge Diagnostics, Inc.
BDS	Bridge Design Specifications
C_b	Moment Gradient Factor
CS	Campbell Scientific
DAQ	Data Acquisition System
F_{cr}	Critical Stress
FEM	Finite Element Method
FHWA	Federal Highway Administration
LRFD	Load and Resistance Factor Design
LTB	Lateral Torsional Buckling
MBE	Manual for Bridge Evaluation
MPH	Miles Per Hour
NCHRP	National Cooperative Highway Research Program
TDOT	Tennessee Department of Transportation

Chapter 1 Goals and Purpose

There are 31 bridges in Tennessee with superstructure systems consisting of steel girders, floor beams, and stringers. The results of TDOT load rating calculations, mandated by FHWA for 30 of these bridges, have shown low capacity (using various methods and software), particularly in the stringers. As a result, an experimental and analytical research program was initiated and focused on a representative bridge in Hardin County.

The research described herein investigated the behavior and capacity of girder-string-floorbeam bridges by:

- Conducting a literature review of the current state-of-practice and emerging research regarding the capacity and behavior of girder-stringer-floorbeam bridges;
- Experimentally measuring strain at various locations and identifying characteristic behavior in the stringers and girders of a representative bridge under live load; and
- Conducting line girder analysis of continuous stringer spans using SIMON software and identifying potential sources of refined load ratings.

Chapter 2 Literature Review

The research team conducted a literature review of the current state-of-practicing and emerging research for live load testing of girder-stringer-floorbeam bridges. The review included previous research published in journals, conferences, and agency reports, both domestic and international. The research team targeted specific publications from the Federal Highway Administration, National Cooperative Highway Research Program, Transportation Research Board, and State Department of Transportation (DOT's).

2.1 Evaluation of a Noncomposite Steel Girder Bridge through Live-Load Field Testing

Breña et al. (2013) conducted research on a damaged noncomposite steel girder bridge in Vermont that consisted of three-span continuous girders. The bridge had previously been damaged through impact of an over-height truck where three of the five girders were affected. The purpose of the research was to measure strain during live-load testing to better understand the bridge behavior and to determine if the damage had detrimental effects on girder capacity.

The bridge supports a 7.5-inch non-composite concrete deck (no shear studs). The total length of the bridge is 214.5 feet with a skew of roughly 42 degrees relative to the abutments. The steel superstructure consists of five W36 X 170 girders spaced at 7.5 feet. Each girder has a 1-inch concrete haunch between the top flange and the deck.

Strain gauges were installed in regions of maximum positive and negative moment within the center span of the bridge, including areas near the piers and at mid-span. Each instrumented section consisted of strain gauges on the bottom of the top and bottom flanges.

Maximum positive and negative moments were generated using two loaded dump trucks, placed 13 feet 5 inches apart, measured rear axle of the front truck to front axle of the trailing truck. To maximize the strain response of various girders, three trucks were placed side-by-side, allowing each truck to straddle one of the interior girders. To calculate the point loads generated by the trucks, the axle weights were determined once the trucks were filled with sand.

Upon evaluation of the load test results, it was noticed that the strains in the top and bottom flanges were asymmetric. Instead of a non-composite strain reading where the top and bottom flanges undergo forces of similar magnitude, the strain in the top flange of the girders was near zero. This indicated that the neutral axis was much higher than it would be if the girders were acting non-compositely.

In regions subject to positive moment during the load test, evidence from the measured strains and neutral axis locations strongly suggest that composite action was occurring between the girders and the deck, even though the bridge was designed to act non-compositely. In areas of negative bending, larger variations of the neutral axis location were observed. However, the location of the neutral axis was high enough to indicate composite behavior between the concrete deck and the girders in sections subject to negative bending.

A 3D Finite Element Method (FEM) model of the bridge superstructure was created to compare with the field results. The girders, diaphragms, and deck were modeled but the piers and abutments were left out due to the girder supports being either pins or rollers and not being necessary to accurately model the bridge. The girders were modeled as composite members by connecting the nodes in the girders to the nodes in the deck with rigid links. Comparisons between the girder moments measured in the field and the calculated moments using FEM modeling were made. The moments measured in the field were similar to those obtained from the FEM results. In nearly all cases studied, the differences between the measured and calculated results did not exceed 18%.

It was concluded that higher flexural capacity of the girders could be considered to allow for trucks larger than what the bridge was originally designed for to pass over.

2.2 Instrumentation During Live Load Testing and Load Rating of Five Slab-on-Girder Bridges

Tomlinson et al. (2016) conducted research on five slab-on-girder bridges for the Maine Department of Transportation. The bridges were originally designed as non-composite (no shear studs) and with the top flange of the girders fully embedded in the concrete deck. The purpose of the research was to assess the degree of unintended composite action between the girders and the deck and to generate recommendations for rating factor modifications based on the results.

Live load testing was performed on each bridge and the results were analyzed and compared with the existing bridge ratings. At mid-span of each bridge, strain gauges were placed on the top and bottom flanges, as well as mid-depth of the web. The gauges were placed on both interior and exterior girders.

Standard three-axle dump trucks were used for the load tests. The trucks were positioned differently depending on the purpose of each individual test. Typically, the trucks were positioned to either produce maximum moment in the girders or a significant amount of shear force.

Three of the bridges resulted in asymmetric strains, much like the research performed by Breña et al. (2013), where the top flange experienced very little strain and the bottom flange experienced a much larger amount. This indicated that the neutral axis was higher than it would be if the girders were acting non-compositely. Two of the bridges resulted in nearly symmetric strains, with both the top flange and bottom flange experiencing large strains. This indicated a neutral axis near mid-depth of the web, much like a non-composite member.

Due to the measured strains near the girder ends on all bridges, it was determined that some degree of rotational restraint was occurring at each abutment. This rotational restraint was likely to have helped limit the strain in the girders at mid-span, leading to a contribution in the overall rating factor increase.

The original non-composite rating factors for the bridges were determined using material properties, load and resistance factors, design live loads, and bridge geometry measured in the field. The results from the load tests were used to compute multiple bridge properties, as well as percent composite action and modified rating factors.

The modified rating factor was computed using a ratio of the computed strain to the measured strain during load testing in accordance with the AASHTO MBE (2010). The equation used to compute the modified rating factor used the standard rating factor and an adjustment factor which incorporated the tests results. The adjustment factor accounts for the difference between the expected response and the measured responses based on load testing. It also accounted for the magnitude of the applied test load and confidence in extrapolating results. The average rating factor increase for the interior and exterior girders was 0.47 and 0.72, respectively.

2.3 Lateral Torsional Buckling Resistance of Continuous Steel Stringers in Existing Bridges

Kuruppuarachchi (2021) conducted research on the flexural capacity of continuous stringers, primarily focusing on the moment gradient factor, C_b. The bridge type studied consisted of two-girder or truss system superstructures with floor beams that are supported by main members and intermediate continuous stringers that are supported by the floor beams.

For bridges of this type, C_b is not accurately calculated in the negative moment region when considering lateral torsional buckling of the stringers. The lateral torsional buckling strength is underestimated due to the bracing effect of the non-composite concrete deck not being accounted for. The purpose of the research was to provide recommendations on how to calculate C_b more accurately.

Lab testing was performed on a two-span structure, consisting of three lines of stringers, steel diaphragms for end supports, and a floorbeam as an interior support. For lateral restraint of the stringers, three options were provided: steel diaphragms, timber struts, and non-composite concrete deck. Variations in the floor beams support, stringer connections to floorbeam, and load cases were provided to investigate the different effects that each condition had on the stringers. Strain gauges were placed along the length of the structure at various locations. Critical locations on the structure were at mid-span and adjacent to the floorbeam.

Finite element analysis was performed on a two-span model to simulate the stringer's behavior while accounting for various loadings and parameters. The model consisted of three continuous stringers supported by a floorbeam, end diaphragms, and a non-composite concrete deck. Two load cases were considered; the interior stringer loaded at one span and the interior stringer loaded at both spans. The area load applied matched the lab test setup. The models were calibrated with the test results to match the testing data regarding the non-composite deck.

It was concluded that the moment gradient factor could be accurately calculated using the equation proposed by Yura and Helwig (2010) and included in the Commentary C-F1-5 of the AISC (2017). The use of this equations results in moment gradient factors that are similar to the finite element analysis results and lab testing data. It also allows for substantial increases in the load ratings of continuous stringers. It was also concluded that the non-composite concrete deck increased the flexural strength of the stringers by approximately 300%.

A representative bridge was used as an example to demonstrate the effects of using the proposed moment gradient factor. Both a concurrent moment approach and a moment envelope approach were used to compare the moment gradient factor and rating factor using the AASHTO LRFD Specifications Art. A6.3.3 method and using the proposed method. Using the moment envelope approach, C_b was increased by 1.39 by using the Yura and Helwig (2010) equation. Using the concurrent moment approach, C_b was increased by 2.4 using the same method. The corresponding rating factors were increased by 0.69 and 0.77 using the moment envelope and concurrent moment approaches, respectively.

2.4 Relevance of Reviewed Articles

The research performed by Breña et al. (2013) and Tomlinson et al. (2016) pertained to steel bridges with a non-composite concrete deck, similar to that of the bridge studied in this research. Both research projects performed live-load testing to determine the strain profile in the cross-sections of the instrumented members. The strain profiles were observed to be asymmetric with the strain in the top flange being much lower than that of the bottom flange. With the results from the load testing, it was determined that a higher flexural capacity of the steel members could be accounted for than what was originally thought. Tomlinson et al. (2016) utilized the load testing results using the AASHTO MBE, which produced a modified rating factor for the bridge members and is also the same method that was used in the research on the SR-114 bridge over the Tennessee River.

Kuruppuarachchi (2021) also conducted research on the flexural capacity of steel bridge members, specifically continuous stringers, and focused on the moment gradient factor, C_b. The results of this research were determined to be useful to the SR-114 bridge over the Tennessee River and were implemented in the final Excel spreadsheet.

Chapter 3 Experimental Test Process

3.1 Instrumentation

3.1.1 General Strain Gauge Locations

Testing of the Billy Nance Memorial Highway Bridge (36-SR114-03.22 / 36SR1140001) was conducted on the North end of the bridge between the north abutment and Pier 15. Strain gauges were placed on the bridge at the general locations shown in Figure 3-1. The stringer/girder/cross-frame configuration is shown in Figure 3-2 (a one-half section of the bridge).

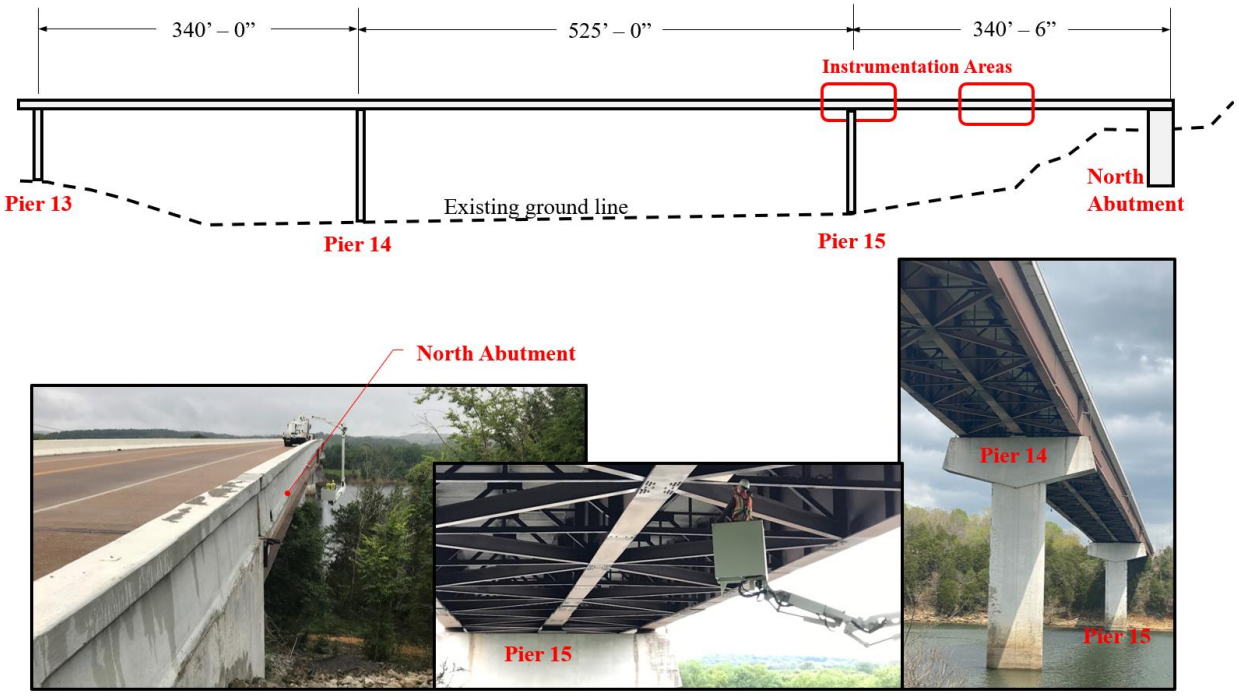

Figure 3-1. General Strain Gauge Placement

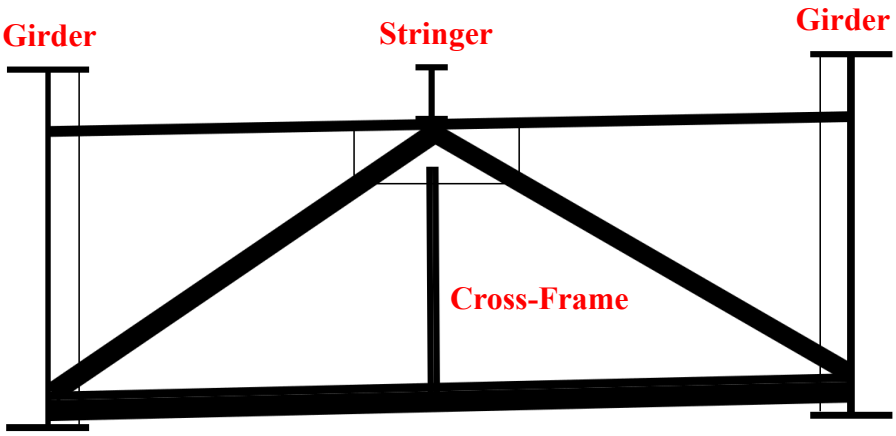

Figure 3-2. Bridge Member Configuration

Gauges were positioned on stringers and girders at the specific locations shown in Figure 3-3. These locations were chosen to record combinations of both local and global bending in the stringers. The stringers and girders span between cross-frames as shown in Figure 3-2, and the girder/stringer/cross-frame system spans between Pier 15 and the abutment. This produces global and local bending of the stringer as shown in the moment diagrams of Figure 3-3. As a result, strain readings at Locations 1, 2, 3, and 4 capture flexural behavior as indicated in Table 3-1 below.

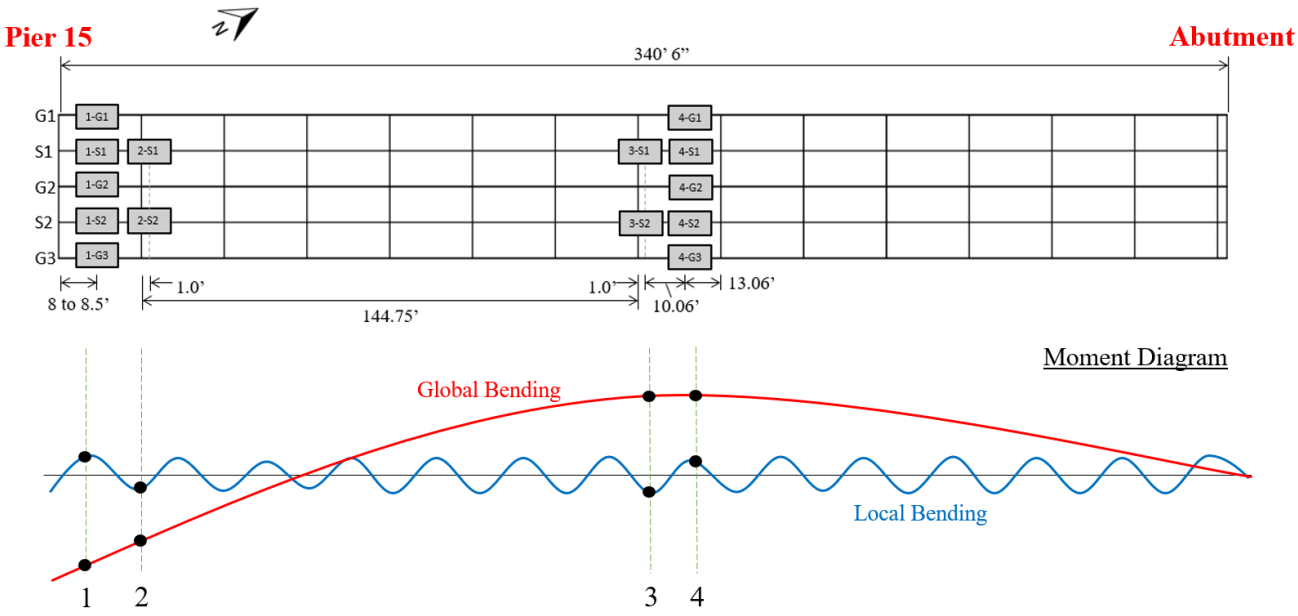

Figure 3-3. Global and Local Bending of Stringers

Table 3-1. Gauge Location and Behavior

Gauge Location and Behavior	
Location	**Flexural Behavior**
1	Global Negative / Local Positive
2	Global Negative / Local Negative
3	Global Positive / Local Negative
4	Global Positive / Local Positive

3.1.2 Specific Strain Gauge Placement on Stringers and Girders

All instrumentation equipment (i.e., strain gauges and the associated data acquisition system (DAQ)) were placed under the bridge using a reach-all vehicle as shown in Figure 3-4. Gauges were placed on the top and bottom flanges as well as the center of the web for both stringers and girders (shown in Figure 3-5) to capture the flexural strain profile throughout the cross-section and, thus, to determine the location of the neutral axis. This information is helpful in determining the level (degree) of composite action between the supporting flexural elements and the concrete bridge deck.

Figure 3-4. Reach-all

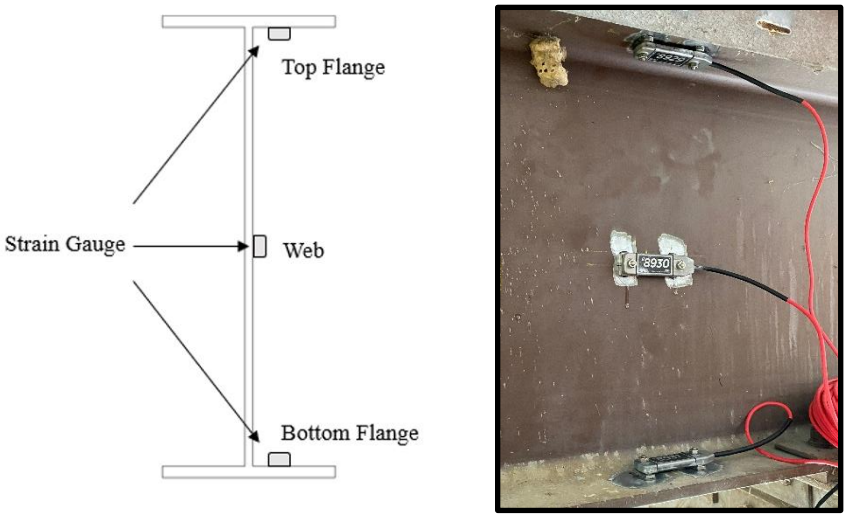

Figure 3-5. Strain Gauge Placement on Typical Stringer

The majority of the gauges were placed to record uniaxial strain resulting from flexure. However, one set of three gauges was also installed on a girder in a rosette fashion in order to determine shear strain at that location (see Figure 3-6). The three gauges (measuring uniaxial strain) produce a horizontal, vertical, and diagonal (45 degree) strain measurement which allows for the analytical solution of the coordinate strains (ε_x, ε_y, and γ_{xy}) in the girder.

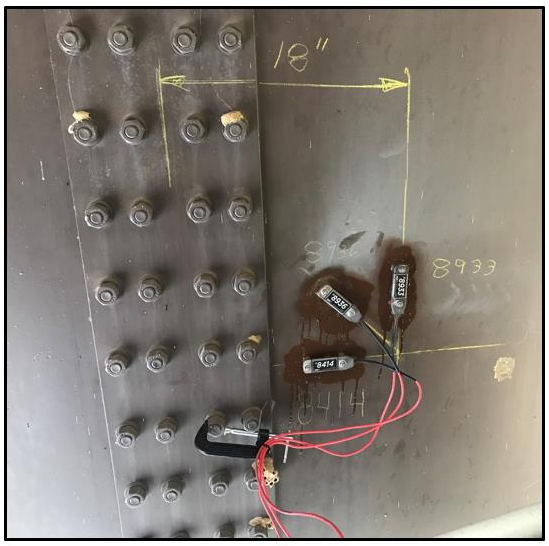

Figure 3-6. Shear Strain Measurement

3.1.3 Strain Gauge Placement Method and Connection to the Data Acquisition System

Strain values at center span (i.e., gauge locations 3 and 4 from Figure 3-3) were considered by the research team to be the most critical and, therefore, were placed first. The installation of the three gauges on each stringer was accomplished simultaneously due to the shallow depth of the stringer and the close proximity of the gauges. The installation procedure (see Figure 3-7) consisted of finding the horizontal and vertical location of the gauges, grinding (i.e., paint removal to bare steel) and cleaning the member, attaching the gauge with epoxy, and painting the connection location (to prevent rust). The procedure was similar for the girders except that gauges were installed individually due to the depth of the girder.

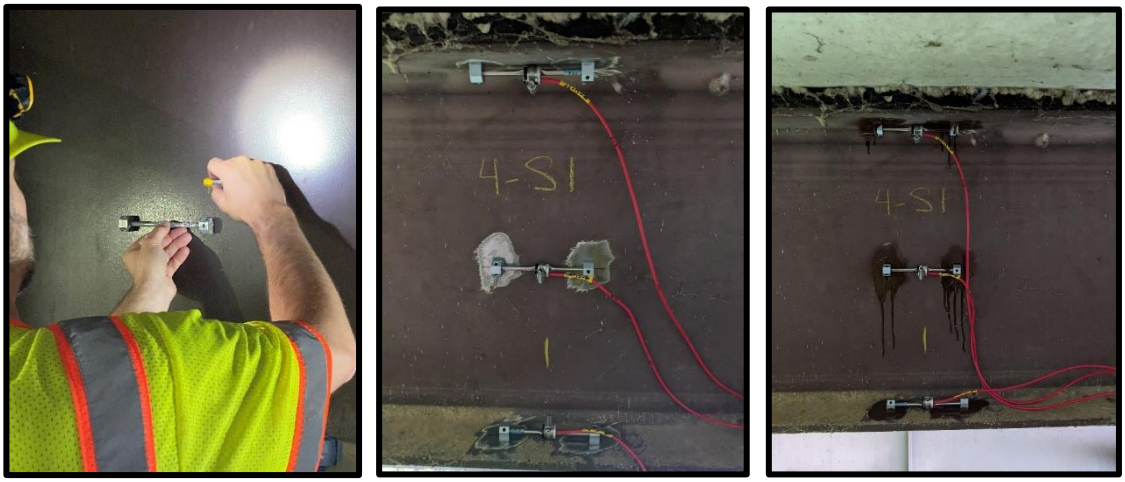

Figure 3-7. Strain Gauge Placement

Cabling for each gauge came in spools that were unwound and clamped intermittently to the bridge structure (usually to a stringer or girder flange) as shown in Figure 3-8. The cable was ultimately connected to a Campbell Scientific (CS) DAQ (consisting of a CS Granite 9 main module and strain module). Two DAQ locations were necessary, one at Pier 15 (top of the pier; see Figure 3-8) and one at mid-span (supported by a field-constructed support platform).

Figure 3-8. Cabling and DAQ Connection

The mid-span gauges as well as the DAQ and support structure were installed and connected by the end of the first day (Monday, July 18th, 2022). The installation of gauges and the DAQ located near Pier 15 were installed and connected by the end of the third day (Wednesday, July 20th, 2022). After completion, the system was tested (by monitoring normal traffic loads) and the output data checked for anomalies.

3.2 Testing

3.2.1 Truck Dimensions and Axle Weights

Standard five-axle TDOT dump trucks, shown in Figure 3-9, were used for the load testing. The total truck weight (i.e., ticket weight) was recorded for each truck (on Thursday, July 21st, 2022) and then was verified using scales placed under each of the truck wheels.

Figure 3-9. TDOT Five Axle Dump Truck

The two middle axles were found to be inconsistent with the pressure they applied to the wheels. As a result, they were raised and disregarded in the weighing and load testing. Truck dimensions (the same for all trucks) were measured at the loading site and consisted of the dimensions shown in Figure 3-10. The recorded weights for the three axles for each truck are listed in Table 3-2.

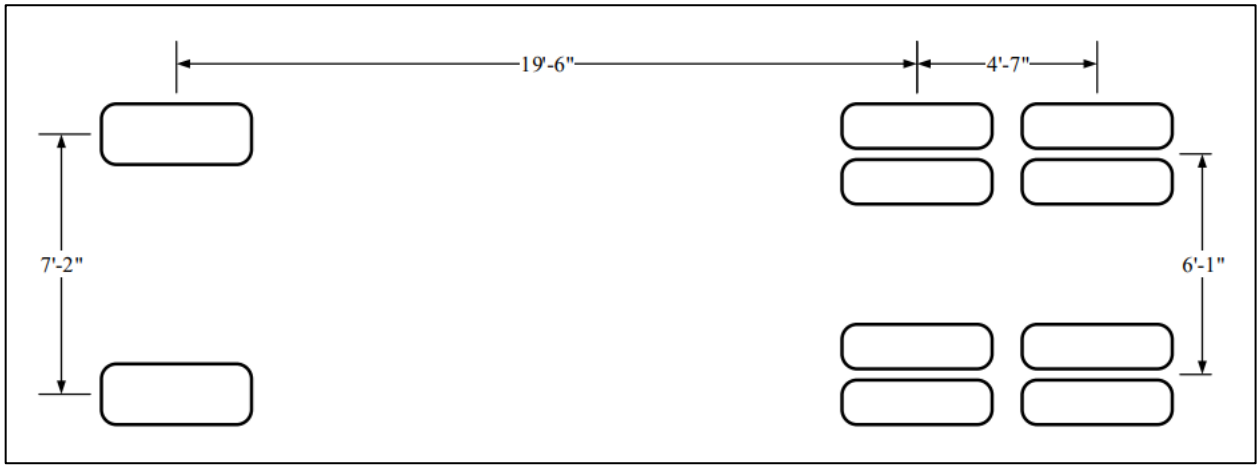

Figure 3-10. Truck Dimensions

Table 3-2. Truck Axle Weights

Truck Axle Weights			
Truck	**Front**	**Middle**	**Back**
A	19,150	21,650	20,650
B	20,300	20,700	20,600
C	18,050	21,350	21,150
D	18,000	21,600	21,450

3.2.2 Truck Load Placement and Sequence

The load testing consisted of four different tests (see Figure 3-11 through Figure 3-14), each with different truck locations to maximize negative and positive moments.

Load Test A utilized two trucks placed on one side of the centerline of the bridge. The wheel nearest to the parapet on Truck B was positioned 3 feet-8 inches from the bottom of the parapet. The wheel on Truck A nearest to Truck B was positioned 4 feet from the centerline of the wheel on Truck B

Load Test B utilized four trucks, separated into two groups. Each group had both trucks positioned into the same orientation as load test A.

Load Test C utilized three trucks, positioned in the middle of the bridge. To position the two outer trucks symmetrically, the outermost wheel of the two outside trucks were positioned 9 feet-3 inches from the bottom of the parapet, and the middle truck was positioned evenly between the two.

Load Test D utilized two trucks positioned in the same way as the outer trucks in load test three.

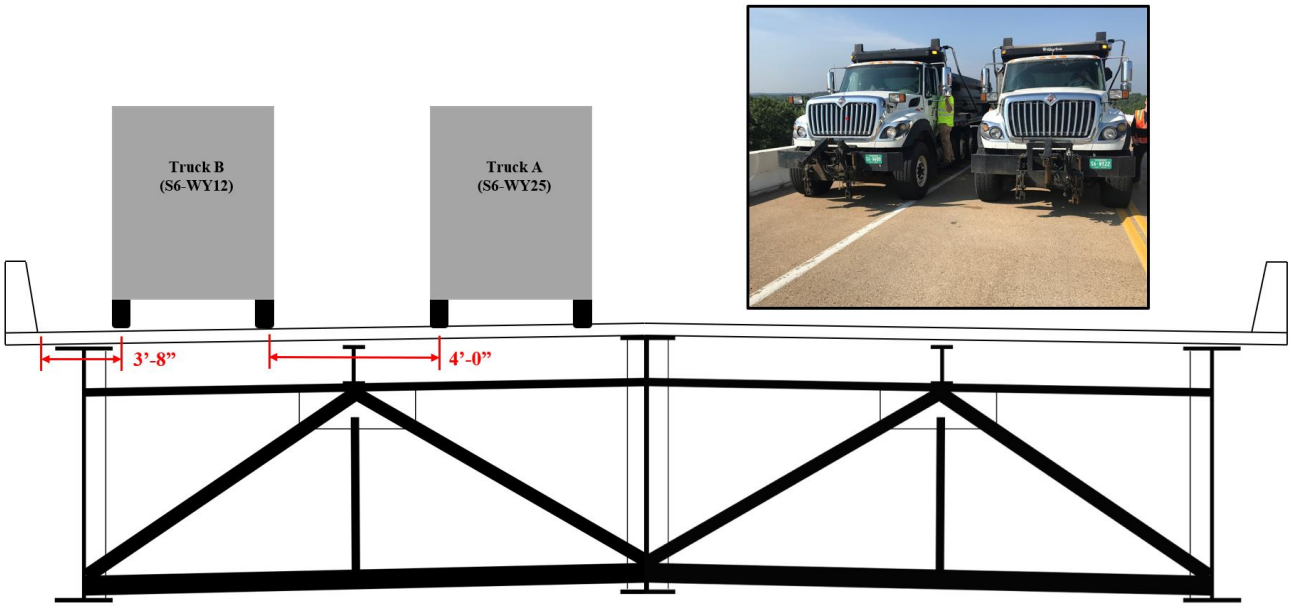

Figure 3-11. Load Test A

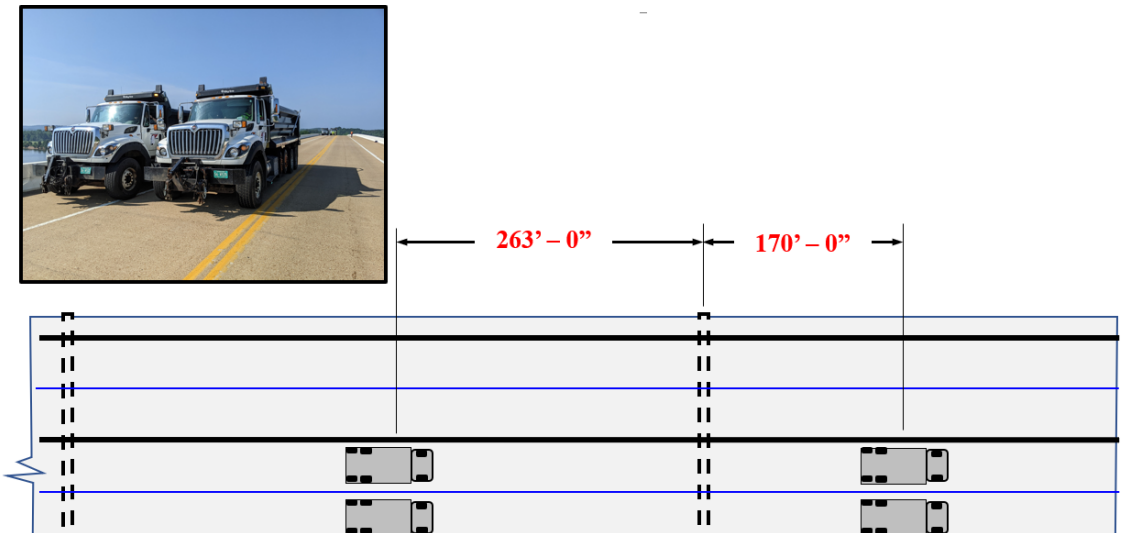

Figure 3-12. Load Test B

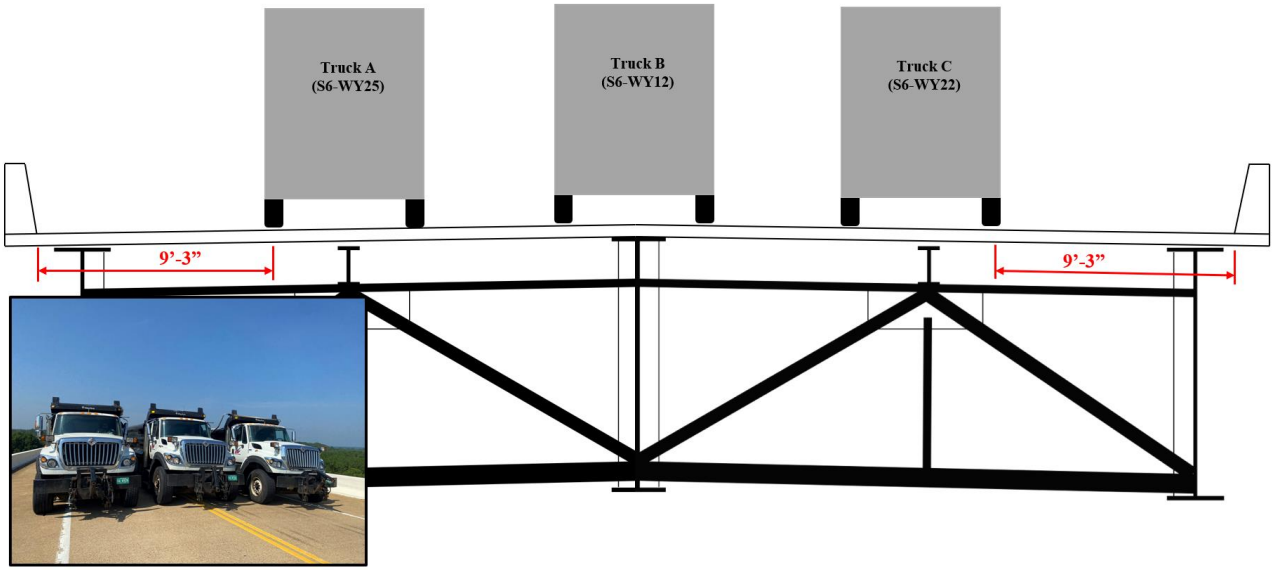

Figure 3-13. Load Test C

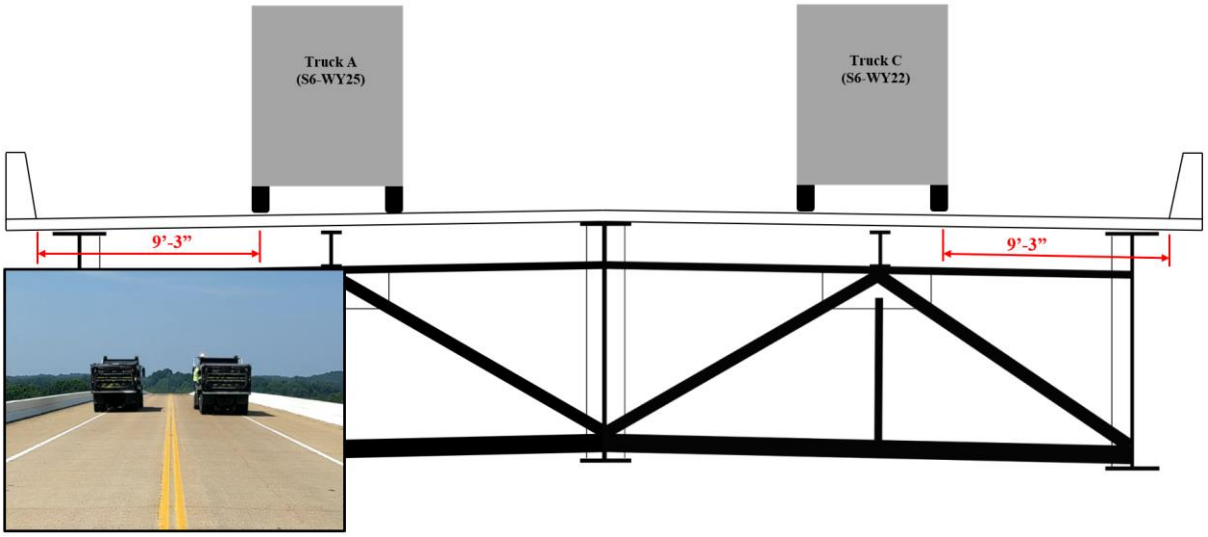

Figure 3-14. Load Test D

3.2.3 Bridge Loading

Each test began by placing the trucks outside of the steel portion of the bridge so that they did not prematurely affect the strain readings. Once the trucks were moved into position, a lead truck was established and a speed between 5 and 10 miles per hour was maintained during the test. The other truck(s) traveled at roughly the same speed as the lead truck while maintaining the proper separation. The trucks completed one crossing of the bridge and then repeated the test while driving back (i.e., maintaining the same positioning).

Load Tests A, C, and D were quasi-static tests (i.e., very slow movement of load across the structure). Load Test B was similar except that the first two trucks parked at the mid-span of pier 15 and the end of the bridge, and the second two trucks parked at the mid-span of Piers 14 and 15. The purpose of Load Test B was to induce maximum negative moment over Pier 15.

3.3Data Processing and Test Results

3.3.1 Introduction

The AASHTO MBE allows for the use of a modified bridge rating factor, RF_T, that may be determined by a factor, K, multiplied by the predicted (i.e., computed) rating factor, RF_C, as follows:

$$RF_T = RF_C(K)$$ 3-1

The factor, K, depends, in part, on measured strains in the test structure. The process for this calculation is examined in detail in Chapter 4. However, as an introduction to Chapter 4, a short summary follows here (concentrating on an explanation of how the test strains, ε_{T1} and ε_{T2}, are used in the MBE calculation for each load test).

3.3.2 Load Test Strains associated with MBE K-Factor

For Load Test A, the maximum and minimum strain readings (see Figure 3-15) for each gauge during the load tests were found and recorded (in Excel). ε_{T1}, the maximum absolute value strain for each cross section (XS1, XS2, XS3, & XS4), and ε_{T2}, the maximum range of strain (i.e., maximum strain minus minimum strain), was found for each gauge, for each cross section.

ε_{T1} and ε_{T2} were then used to calculate the K factor for each cross section as prescribed by the MBE, and the strain values corresponding to the minimum K value (controlling K) were determined.

This process was repeated for each of the remaining load tests (B through D), with values shown in Figure 3-15 through Figure 3-18.

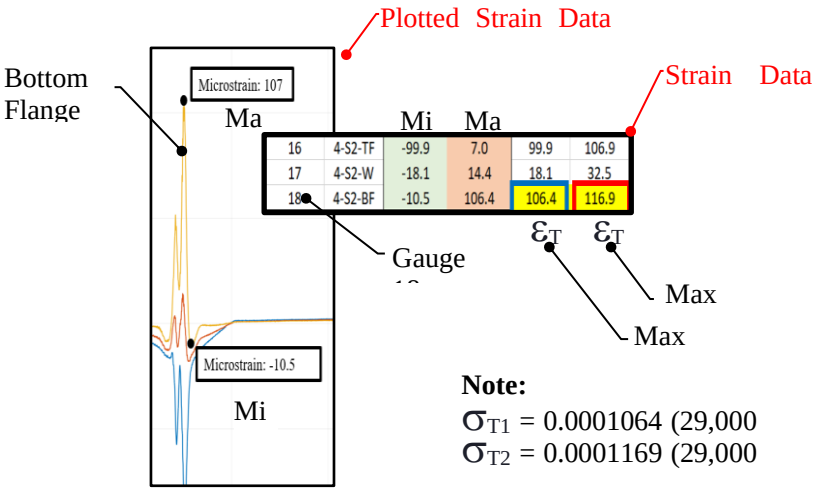

Load Test	Cross-Section	ε_{T1}	ε_{T2}	1-Lane M ft-k	1-Lane ΔM ft-k	mg Lanes	ε_{C1}	ε_{C2}	$\varepsilon_{C1}/\varepsilon_{T1}$	$\varepsilon_{C2}/\varepsilon_{T2}$	K_a	K	K_{min}
A	XS1	74	87	115.7	148.0	0.928	273	350	3.696	4.021	2.696	2.348	1.766
	XS2	79	89	101.1	133.4	0.928	239	315	3.025	3.543	2.025	2.013	
	XS3	82	85	101.1	133.4	0.928	239	315	2.914	3.710	1.914	1.957	
	XS4	107	117	114.6	141.2	0.928	271	334	2.532	2.853	1.532	1.766	

Figure 3-15. Strain and K-factor Calculation for Load Test A

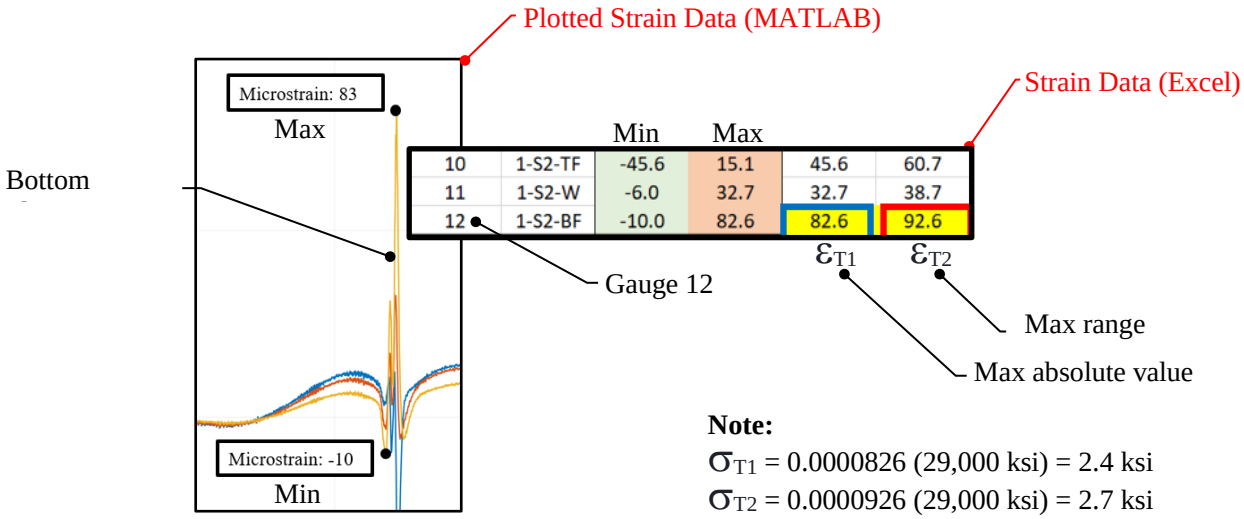

B	XS1	83	93	115.7	148.0	0.928	273	350	3.295	3.762	2.295	2.148	
	XS2	75	90	101.1	133.4	0.928	239	315	3.186	3.504	2.186	2.093	2.093
	XS3	56	61	101.1	133.4	0.928	239	315	4.268	5.169	3.268	2.634	
	XS4	23	26	114.6	141.2	0.928	271	334	11.778	12.837	10.778	6.389	

Figure 3-16. Strain and K-factor Calculation for Load Test B

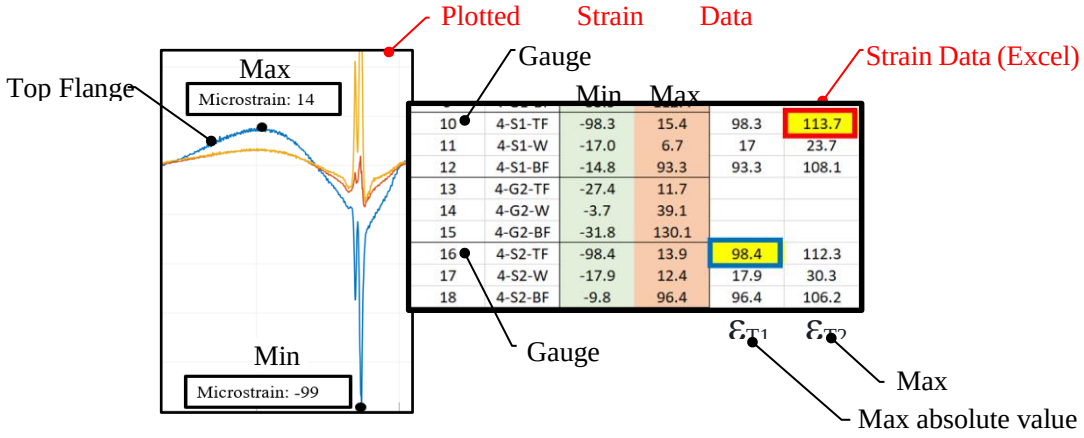

C	XS1	81	96	115.7	148.0	0.828	244	312	3.013	3.252	2.013	2.006	
	XS2	72	85	101.1	133.4	0.828	213	281	2.962	3.310	1.962	1.981	1.721
	XS3	78	92	101.1	133.4	0.828	213	281	2.734	3.058	1.734	1.867	
	XS4	99	114	114.6	141.2	0.828	242	298	2.441	2.612	1.441	1.721	

Figure 3-17. Strain and K-factor Calculation for Load Test C

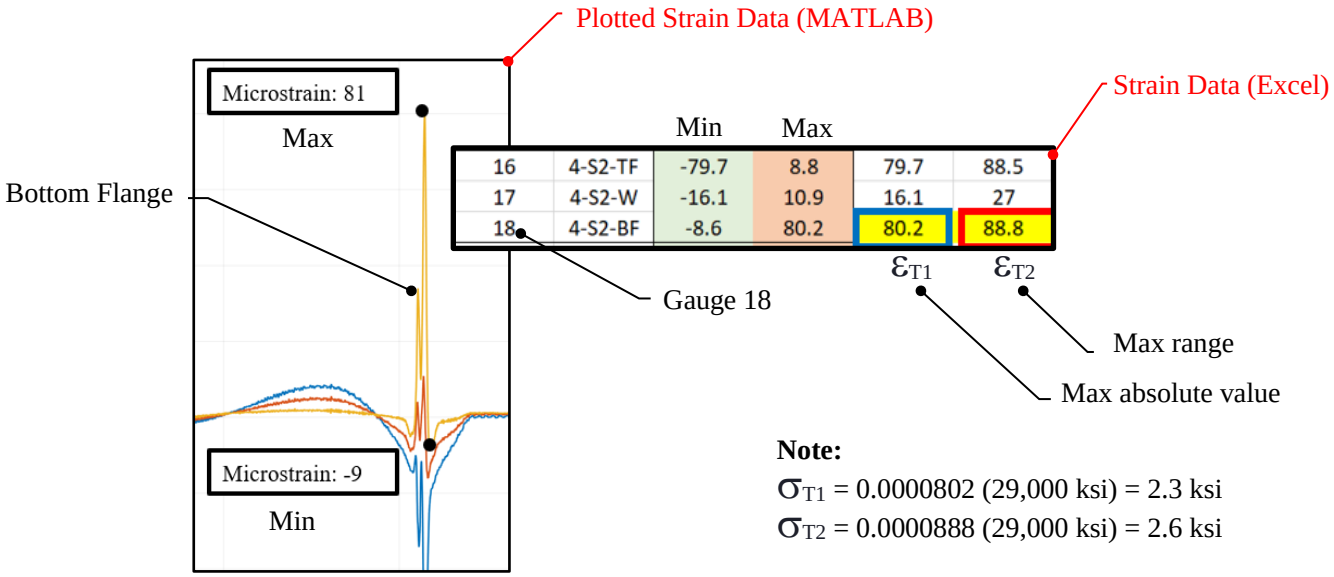

D	XS1	73	84	115.7	148.0	0.656	193	247	2.648	2.944	1.648	1.824	
	XS2	63	71	101.1	133.4	0.656	169	223	2.682	3.140	1.682	1.841	1.682
	XS3	58	73	101.1	133.4	0.656	169	223	2.913	3.054	1.913	1.956	
	XS4	81	89	114.6	141.2	0.656	191	236	2.364	2.651	1.364	1.682	

Figure 3-18. Strain and K-factor Calculation for Load Test D

Chapter 4 Analytical Evaluation

Eight areas have been identified as potential sources of refined ratings for stringers in girder-stringer-floorbeam bridges. Each of these is discussed in individual section following.

1. Live Load Distribution Factors for Stringers
2. Lateral Torsional Buckling Modification Factor (C_b)
3. Critical Stress (F_{cr}) Calculation
4. Appendix A6 vs. Chapter 6 Provisions
5. Diagnostic Load Testing
6. Low Traffic Volumes
7. Condition and System Factors
8. Wearing Surface Elimination

In addition, a final section on Conclusions and Recommendations is included.

4.1 Live Load Distribution Factors for Stringers

The AASHTO LRFD Bridge Design Specifications (BDS), in Chapter 4, provide equations for live load distribution factors on bridge girders analyzed and designed using line-girder, continuous beam analysis. The applicability of these equations to stringers in girder-stringer-floorbeam bridge construction is questionable. Hence, software packages often adopt the lever rule for live load distribution under such conditions.

The lever rule is the method adopted in SIMON to determine shears and moments in the stringers from a line girder analysis for the bridge geometries studied in this project. The lever rule distribution factors for the SR-114 bridge over the Tennessee River are given in Equations 4-1 and 4-2 for single lane and multiple lane conditions, respectively. The 1.2 factor in Equation 4-1 is the multi-presence factor, *m*, for a single lane loaded.

$$mg = 1.2\left(\frac{S-3}{S}\right) = 1.2\left(\frac{10.417-3}{10.417}\right) = 1.2(0.712) = 0.854\ Lanes/stringe \quad \textbf{4-1}$$

$$mg = 1.0\left(\frac{2S-10}{S}\right) = 1.0\left(\frac{2\times 10.417-10}{10.417}\right) = 1.04\ Lanes/stringe \quad \textbf{4-2}$$

The AASHTO MBE, in Article 6A.2.3.2, provides the following.

"Utilizing the number and transverse placement of lanes in accordance with AASHTO LRFD Bridge Design Specifications may not be consistent with the actual usage of the bridge as defined by the striped lanes and could result in conservative load ratings for bridge types such as trusses, two-girder bridges, arches, and exterior girders, where live load distribution factors are established using the lever rule method. Upon the approval of the bridge owner, an alternate load rating of the bridge for normal operating conditions or current usage may be performed by placing truck loads only within the striped lanes. When load rating a structure based on the existing striped lanes, the transverse positioning of the truck should include placing the wheel load anywhere within the lane, including on the lane stripe. This alternate load rating may be performed for all live load models. Placement of striped lanes on the bridge should be field verified and documented in the inspection report."

It seems reasonable to determine distribution factors based on actual striped lanes, if the Owner approves, and if the lane placement is field verified and documented in the bridge inspection report.

For the SR-114 bridge over the Tennessee River, with a single stringer on each side of the centerline and a single striped lane on each side of the centerline, the use of a striped lane distribution factor corresponding to Equation 4-1 could be applied. For cases in which a stringer is located near the common edge of two striped lanes, the application of a striped-lane distribution factor should not be applied – the design distribution factor given by Equation 4-2 should be used in such cases.

4.2 Lateral-Torsional Buckling Modification Factor (C_b)

Standard C_b-calculation for typical bridge members is based on discrete brace points. Equation 4-3 presents the equation adopted in the AASHTO BDS. SIMON software was used to model a three-span continuous stringer and the resulting factors were $C_b = 1.75$ for end spans ($f_1/f_2 = 0$) and $C_b = 1.00$ for interior spans ($f_1/f_2 = 1$).

$$C_b = 1.75 - 1.05\left(\frac{f_1}{f_2}\right) + 0.3\left(\frac{f_1}{f_2}\right)^2 \leq 2.30 \qquad \textbf{4-3}$$

However, for stringers in girder-stringer-floorbeam bridges, the structural boundary conditions are likely similar to those depicted in Figure 4-1, taken from the AISC Manual for Steel Construction. Equation 4-4 is from the AISC Commentary and has been deemed appropriate for stringers in bridges in the literature.

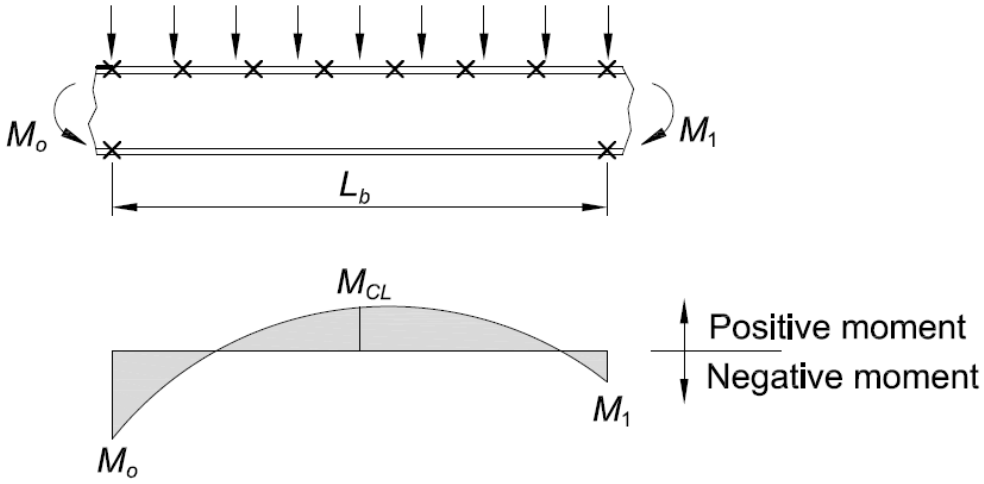

Figure 4-1. Stringer Boundary Conditions (AISC)

$$C_b = 3.0 - \frac{2}{3}\left(\frac{M_1}{M_o}\right) - \frac{8}{3}\left[\frac{M_{CL}}{(M_o + M_1)^*}\right] \qquad \textbf{4-4}$$

In Equation 4-4, M_o is the end moment for the unbraced length which causes the largest compressive stress in the bottom flange. M_1 is the other end moment. M_{CL} is the moment at mid-span. Moments are taken as positive if causing tension in the bottom flange, negative if causing compression in the bottom flange. The quantity $(M_o + M_1)^*$ is taken to be equal to M_o in cases where M_1 is positive.

For the SR-114 bridge over the Tennessee River, the resulting C_b-factors upon application of Equation 4-4 are $C_b = 2.76$ for an end span and $C_b = 2.08$ for an interior span. These values were calculated from moment envelopes, and the literature suggests that a 15% increase in the values may be appropriate when moment envelopes are used in the analysis of C_b.

It seems clear that, provided the top flange boundary condition shown in Figure 4-1 accurately represents stringers in girder-stringer-floor beam bridges, default C_b-factors are overly conservative, and Equation 4-4 should be used to obtain accurate ratings.

4.3 Critical Stress (F_{cr}) Calculation

The critical stress in lateral torsional buckling (LTB), F_{cr}, is a key parameter in the rating of stringers in girder-stringer-floorbeam bridges. Equation 4-5 gives the expression for F_{cr} taken from Chapter 6 (Equation 6.10.8.2.3-8) of the AASHTO BDS. Equation 4-6 is the expression for the same parameter as presented in both Appendix A6 (Equation A6.3.3-8) of the AASHTO BDS and Article F2.2 of the AISC Manual of Steel Construction. The term under the radical in Equation 4-6 is hereafter referred to as the "F_{cr}-Modifier". Apparently, the form given by Equation 4-6 for F_{cr} is more appropriate for rolled shapes, such as stringers, while Equation 4-5 is more appropriate for deep, welded plate girders. Bridge software likely does not include

the F_{cr}-Modifier. For example, SIMON neglects the F_{cr}-Modifier in calculations. This is a clear source of unnecessary conservatism and application of the F_{cr}-Modifier is appropriate for the rating of stringers. For the W24x68 stringers on the SR-114 bridge over the Tennessee River, the F_{cr}-Modifier is equal to 1.30 (30% increase in the critical stress).

$$F_{cr} = \frac{C_b \pi^2 E}{(L_b/r_t)^2} \quad \textbf{4-5}$$

$$F_{cr} = \frac{C_b \pi^2 E}{(L_b/r_t)^2} \sqrt{1 + 0.078 \frac{J}{S_{xc} h} \left(\frac{L_b}{r_t}\right)^2} \quad \textbf{4-6}$$

4.4 Appendix A6 Provisions vs. Chapter 6 Provisions

For rating at the Strength limit state, Article 6A.6.9.1 of the MBE requires that Article 6.10.8 of the LRFD BDS is to be used in establishing flexural resistance for non-composite sections. With an unbraced panel length of 25 feet, it is anticipated that the nominal Strength limit state moment in steel stringers of girder-stringer bridges must be limited to that given by Equation 4-7, provided Equation 4-8 is satisfied. This should be checked for the stringers on a given project, but the anticipation is that local buckling will not control (the condition is satisfied at $F_y \leq 50$ ksi for all stringers studied in this project: W18 x 50, W18 x 55, W18 x 60, W24 x 68). Further assuming that the actual unbraced length is greater than L_r, as is the case with all stringers included in this study, the flexural resistance in accordance with AASHTO 6.10.8 is given by Equation 4-7.

$$M_n = F_{cr} S_x \leq F_y S_x \quad \textbf{4-7}$$

$$\lambda_f = \frac{b_f}{2t_f} \leq \lambda_{pf} = 0.38 \sqrt{\frac{E}{F_y}} \quad \textbf{4-8}$$

Further benefit in obtaining an accurate load rating of stringers may be possible, in some cases, by applying Appendix A6 of the LRFD Bridge Design Specifications. In fact, the Commentary to Article 6.10.8.1.1 encourages the use of Appendix A6 for straight members with compact webs and F_y no greater than 70 ksi. Appendix A6 permits plastification of the web in adequately braced, compact sections. Moment resistance for such conditions may reach the plastic moment, whereas Chapter 6 limits the resistance to the yield moment. In properly design members, the application of load factors means that the plastic moment will never be reached, even though the resistance is taken as the plastic moment.

To qualify for the application of Appendix A6 provisions, the stringer must satisfy Equation 4-9. Given that the stringers are non-composite for analysis, D_c and D_{cp} are both equal to one-half of the web depth for the rolled sections. Rolled W-shape stringers with F_y no greater than 70 ksi automatically satisfy additional criteria for compactness in Appendix A6. The primary benefit possible by using Appendix A6 is the web plastification potentially permitted in flexural resistance. For stringers satisfying Equation 4-10, the web plastification factor R_p, may be taken from Equation 4-11. Otherwise, R_p is given by Equation 4-12. Note that the equations presented here have been simplified from the format given in Appendix A6 to incorporate the doubly symmetric, non-composite nature of the subject stringers. F_{cr} and M_n may then be determined using Equations 4-16 and 4-17, respectively. Appendix A6 does limit C_b to no more than 2.3. Much higher values have been reported in the literature for boundary conditions corresponding to those in the stringers of girder-stringer-floorbeam bridges, however.

$$\lambda_w = \frac{h}{t_w} \leq \lambda_{rw} \qquad \textbf{4-9}$$

$$\frac{h}{t_w} \leq \lambda_{pw(Dcp)} \qquad \textbf{4-10}$$

$$R_p = \frac{M_p}{M_y} = \frac{Z_x}{S_x} \qquad \textbf{4-11}$$

$$R_p = \left[1 - \left(1 - \frac{S_x}{Z_x}\right)\left(\frac{\lambda_w - \lambda_{pw(Dcp)}}{\lambda_{rw} - \lambda_{pw(Dcp)}}\right)\right]\frac{Z_x}{S_x} \leq \frac{Z_x}{S_x} \qquad \textbf{4-12}$$

$$4.6\sqrt{\frac{E}{F_y}} \leq \lambda_{rw} = \left(3.1 + \frac{5.0}{a_{wc}}\right)\sqrt{\frac{E}{F_y}} \leq 5.7\sqrt{\frac{E}{F_y}} \qquad \textbf{4-13}$$

$$a_{wc} = \frac{ht_w}{b_f t_f} \quad \textbf{4-14}$$

$$\lambda_{pw(Dcp)} = \frac{\sqrt{E/F_y}}{\left(0.54\frac{Z_x}{S_x} - 0.09\right)^2} \leq \lambda_{rw} \quad \textbf{4-15}$$

$$F_{cr} = \frac{C_b \pi^2 E}{(L_b/r_t)^2}\sqrt{1 + 0.078\frac{J}{S_{xc}h}\left(\frac{L_b}{r_t}\right)^2} \quad \textbf{4-16}$$

$$M_n = F_{cr}S_x \leq R_{pc}M_y \quad \textbf{4-17}$$

So, it is evident that in some situations, Appendix A6 permits the nominal resistance to correspond to the plastic resistance while Chapter 6 limits the nominal resistance for such systems to the yield resistance. Note that F_{cr} is not limited to values less than F_y in Appendix A6.

4.5 Diagnostic Load Testing

Article 8.8.2.3 of the MBE provides the required means of adjusting a rating factor when comparing predicted and measured response. For the current project, predicted versus measured response is envisioned to be primarily that relating to live load distribution.

Following a diagnostic load test, a modified rating factor, RF_T, may be computed from the predicted rating factor, RF_C, according to the equation presented here as Equation 4-18.

$$RF_T = RF_C(K) \quad \textbf{4-18}$$

$$K = 1 + K_a K_b \quad \textbf{4-19}$$

$$K_a = \frac{\varepsilon_C}{\varepsilon_T} - 1 \qquad \textbf{4-20}$$

The adjustment factor, *K*, depends on two other factors, K_a and K_b, as shown in Equation 4-19. K_a depends on the ratio of predicted (ε_C) to measured strains (ε_T) in the element under consideration, may be positive or negative, and is given by Equation 4-20. K_b is intended to account for the analytical program and the team's understanding of potential load capacity enhancements. Table 4-1 is taken from *Section 8.8.2.3.1* of the *MBE* and should be used for guidance in establishing appropriate values for K_b. The rating vehicle weight is *W,* and the test vehicle weight is *T* in the table.

Table 4-1. Values for K_b in the MBE

Can behavior be extrapolated to 1.33*W*?		Magnitude of Test Load			K_b
Yes	No	*T/W* < 0.4	0.4<*T/W*<0.7	*T/W* > 0.7	
√		√			0.00
√			√		0.80
√				√	1.00
	√	√			0.00
	√		√		0.00
	√			√	0.50

Based on discussions among the research team and the TDOT personnel for the project, a value of K_b = 0.50 has been deemed appropriate for the rating of stringers.

The basis for this decision is twofold: (a) the diagnostic load test was completed using four trucks, each about 62 kips in weight (T/W = 62 / 72 = 0.86 > 0.70) and (b) extrapolation beyond 1.33W = 1.33 x 72 = 96 kips was not permitted.

The controlling ratio of ε_C / ε_T for the SR-114 load test was found to be 2.38 resulting in a K-factor equal to 1.68.

For stringers in bridges deemed essentially the same as those on SR-114 over the Tennessee River, a K-factor equal to 1.68 may be used to establish stringer ratings. For other cases, additional diagnostic testing, like that employed here, is recommended.

4.6 Low Traffic Volumes

Load factors applicable for steel bridges for each rating level are summarized in Table 4-2, taken directly from the MBE, Article 6A.4.4.2.

Table 4-2. MBE-Specified Load Factors

Limit State	Dead Load	Dead Load	Design Load		Legal Load
			Inventory	Operating	
	γ_{DC}	γ_{DW}	γ_{LL}	γ_{LL}	γ_{LL}
Strength I	1.25	1.50	1.75	1.35	1.45[a] 1.45[b]
Service II	1.00	1.00	1.30	1.00	1.30
Fatigue I	0.00	0.00	1.75	-	-
Fatigue II	0.00	0.00	0.80	-	-

[a] Value shown is applicable for routine commercial traffic and is dependent on ADTT. See the *MBE* Table 6A.4.4.2.3a-1 for reduced values when ADTT is less than 5000.

[b] Value shown is applicable for specialized hauling vehicle and is dependent on ADTT. See the *MBE* Table 6A.4.4.2.3b-1 for reduced values when ADTT is less than 5000

For both routine commercial traffic and for specialized hauling vehicles, the load factor may be reduced from 1.45 to 1.30 when the ADTT is no more than 1,000. For ADTT between 1,000 and 5,000 interpolation may be used to determine the appropriate load factor on legal load and specialized vehicle rating procedures.

4.7 Condition and System Factors

The general load rating equation is found in *Article 6A.4.2.1* of the *MBE* and is repeated here as Equation 4-21.

$$RF = \frac{C - \gamma_{DC}DC - \gamma_{DW}DW \pm \gamma_P P}{\gamma_{LL}(LL + IM)} \quad \textbf{4-21}$$

$$C = \phi_c \phi_s \phi R_n \quad \textbf{4-22}$$

$$\phi_c \phi_s \geq 0.85 \qquad \textbf{4-23}$$

The γ values are load factors and ϕ's are resistance factors for condition, system, and LRFD-based resistance. R_n is the LRFD-based nominal resistance.

Table 6A.4.2.4-1 of the *MBE* specifies a system factor, ϕ_s, equal to 1.00 for redundant stringer subsystems. This value is judged to be appropriate for the stringers in TDOT girder-stringer bridges. However, the commentary to Article 6A.4.2.4 states that more accurate system factors from *NCHRP Report 406* (Ghosn & Moses, 1998) may be used. Table 4-3, for continuous steel I-beam bridges, is reproduced from *NCHRP Report 406* and may prove useful in the accurate rating of stringers in TDOT girder-stringer bridges. Note the span limit for the tables is stated to be 45 to 150 feet, which further complicates the use of system factors from the report. Further research would be required to justify system factors greater than 1.0.

For each configuration, use the lowest value from the ultimate, functionality, and damage limit states.

The values shown in the table for the damage limit state shall be increased by 0.10 for bridges with a distributed set of diaphragms.

A minimum value of 0.80 shall be used.

A maximum value of 1.20 shall be used.

Condition factors, ϕ_c, will be assigned by TDOT staff in accordance with *Article 6A.4.2.3* of the *MBE* for bridges to be evaluated.

Table 4-3. NCHRP Report 406 System Factors

Spacing	Limit State	4 Beams	6 Beams	8 Beams	10 Beams
4 ft	ultimate	0.83	1.03	1.04	1.03
	functionality	0.95	1.11	1.13	1.13
	damage	1.31	1.47	1.48	1.48
6 ft	ultimate	1.03	1.07	1.06	1.06
	functionality	1.11	1.15	1.15	1.15
	damage	1.25	1.32	1.32	1.32
8 ft	ultimate	1.06	1.07	1.07	1.07
	functionality	1.13	1.15	1.15	1.15

	damage	1.19	1.22	1.22	1.22
10 ft	ultimate	1.06	1.07	1.07	
	functionality	1.15	1.16	1.16	
	damage	1.09	1.10	1.10	
12 ft	ultimate	1.04	1.05		
	functionality	1.14	1.15		
	damage	0.99	0.99		

Refined system and condition factor assessment is beyond the scope of this study. While such issues may benefit TDO in future ratings, additional research would be required to recommend factors greater than 1.0.

4.8 Elimination of Wearing Surface Loading Where Appropriate

For bridges with no wearing surface, more accurate ratings may be obtained by not including those loads in the rating procedure, even though they were likely included in the design of the bridge elements.

Chapter 5 Results and Discussion

Provisions in the AASHTO LRFD Bridge Design Specification, primarily intended to be applied to welded plate girders, are overly conservative for the rating of rolled steel stringers in bridges constructed with deep plate girders, cross-frames, and stringers supported on those cross-frames. The sources on conservatism include the following.

- The exclusion of a modifier on the critical buckling stress, F_{cr}, used in determining flexural resistance results in a significant conservatism.
- The 'default' lateral-torsional buckling modifier, C_b, in typical computer programs, is overly conservative when applied to stringers with top flanges continuously braced, bottom flanges bolted to supporting cross-frames, and inflection points between cross-frames. Based on the literature, including studies at Louisiana Tech (Kuruppuarachchi, 2021) (Sun, et al., 2021) as well as Commentary Section C-F1 guidance from AISC (AISC, 2016), the most appropriate C_b-factor equation is that given by Equation 4-4.

  The use of a 'design' distribution factor based on the lever rule would appear to be overly conservative, given the observed strains in stringers for the load test bridge. It is recommended that the lever rule be used for stringer rating, but additional diagnostic load testing of bridges is recommended where the analytical issues (e.g., Cb, Fcr, striped lane distribution, Appendix A6, etc.) still result in low ratings. Taking $K_b = 0.50$, this results in a modified rating factor equal to 1.69 times that obtained using the procedure described here (design distribution factor by the lever rule). Lever rule distribution factors may be computed using Equation 4-2 for bridges with stringer-to-girder spacing not less than 8 feet.
- If the Owner desires, live load distribution could be based on a striped-lane, lever-rule methodology, provided inspection identifies no distress in the stringers. This methodology is explicitly permitted, with Owner approval, by the Manual on Bridge Evaluation (AASHTO, 2019) in Article 6A.2.3.2. With *S* equal to the lateral spacing between a stringer and adjacent girder (one-half of the spacing between two adjacent girders), the distribution factor is given by Equation 4-1.
- The application of provisions from Appendix A6 of the LRFD Bridge Design Specifications is typically not undertaken in computer programs. The application of such provisions is often permissible and beneficial in the rating of stringers made from rolled steel sections.

Provided inspection shows no signs of distress, the following procedure is recommended for the rating of stringers in TDOT girder-stringer bridges. The procedure is applicable to both design and legal load rating.

1. Perform a line girder analysis to determine maximum Strength, Service, and Fatigue limit state moments, both negative and positive. Distribution factors should be that shown in Equation 4-2 for Strength and Service limit states, and that given by Equation 4-1 without the 1.2 factor for the Fatigue limit state. A three-span model will suffice, even though the stringers are typically continuous over several spans.

2. At the Owner's discretion, use Equation 4-1 to determine an appropriate striped-lane distribution factor in lieu of typical design factors for Strength and Service limit states. Eliminate the overlay allowance if none is present from inspection. Assume parapet loads are carried equally by all longitudinal elements (girders and stringers). Use a reduced load factor for legal loads at the Strength limit state if the ADTT is less than 5,000.
3. Determine an appropriate C_b-factor using Equation 4-4 and the moment envelopes from the line girder analysis at the Strength I limit state. At the Owner's discretion (not recommended), apply the 15% increase in C_b, given that the calculation uses moment envelopes rather than instantaneous moments.
4. Determine F_{cr} using Equation 4-6.
5. Compute λ_w for the web from Equation 4-9 (or use Tables form the AISC Steel Construction Manual to find $\lambda_w = h/t_w$).
6. If λ_w satisfies Equations 4-9 and 4-13, apply Appendix A6 to determine the Strength limit state M_n from Equation 4-17. Otherwise, apply Chapter 6 provisions to find M_n from Equation 4-7. In either case, ensure that Equation 4-8 for the flange is satisfied.
7. Take $M_n = 0.8 \times F_y \times S_x$ at the Service limit state and use Equation 4-21 to establish the Service limit state Rating Factor.
8. Use the maximum and minimum Fatigue limit state moments from the line girder analysis and calculate the factored stress range using a load factor equal to 1.75, corresponding to infinite life fatigue. Use $C = \Delta F_{TH} = 24$ ksi (non-weathering steel) or $C = \Delta F_{TH} = 16$ ksi (weathering steel) to establish the Fatigue limit state Rating factor using Equation 4-21.
9. For completeness, ensure that the Strength limit state shear resistance is satisfactory. AISC Manual tables may be useful for this assessment.
10. If low ratings are still indicated, consider diagnostic load testing of the bridge.

Applying the recommended procedure for the SR-114 bridge over the Tennessee River significantly increases the computed rating factors. Figure 5-1 provides a summary of ratings based on 'default', overly conservative assumptions typically used in software. Figure 5-2 provides a summary of ratings with the following options:

- refined C_b calculation without 15% increase for envelope effects
- application of F_{cr} modifier
- design lane live load distribution
- application of Appendix A6 provisions

Rating calculations were completed using the spreadsheet developed as part of this project: "***Stringer-Rating-1.0Beta.xlsx***".

Strength Limit State Rating Factors					
Model	Load	End Span M^+ RF	Interior Span M^+ RF	End Span M^- RF	Interior Span M^- RF
2-Span	HL-93 Inventory	**0.778**	NA	**0.424**	NA
3-Span	HL-93 Inventory	**0.765**	1.063	**0.209**	**0.209**
2-Span	HL-93 Operating	1.008	NA	**0.549**	NA
3-Span	HL-93 Operating	**0.991**	1.378	**0.271**	**0.271**
2-Span	Type 3 Legal	1.563	NA	1.101	NA
3-Span	Type 3 Legal	1.549	2.132	**0.503**	**0.503**
2-Span	Type 3S2 Legal	1.671	NA	**0.895**	NA
3-Span	Type 3S2 Legal	1.655	2.268	**0.435**	**0.435**
2-Span	Type 3-3 Legal	1.899	NA	1.143	NA
3-Span	Type 3-3 Legal	1.838	2.589	**0.534**	**0.534**
2-Span	Type NRL Legal	1.145	NA	**0.892**	NA
3-Span	Type NRL Legal	1.137	1.586	**0.389**	**0.389**

		Service Limit State Rating Factors		
Model	Load	Positive M_u	RF	RF
2-Span	HL-93 Inventory	496.0	**0.711**	**0.612**
3-Span	HL-93 Inventory	501.6	**0.697**	**0.718**
2-Span	HL-93 Operating	394.9	**0.925**	**0.795**
3-Span	HL-93 Operating	401.2	**0.906**	**0.933**
2-Span	Type 3 Legal	320.9	1.185	1.317
3-Span	Type 3 Legal	325.6	1.170	1.430
2-Span	Type 3S2 Legal	304.0	1.267	1.070
3-Span	Type 3S2 Legal	309.1	1.249	1.236
2-Span	Type 3-3 Legal	274.4	1.440	1.367
3-Span	Type 3-3 Legal	284.9	1.387	1.519
2-Span	Type NRL Legal	416.9	**0.868**	1.067
3-Span	Type NRL Legal	419.6	**0.859**	1.107

Fatigue Limit State Rating Factors		
2-Span	Fatigue	1.051
3-Span	Fatigue	1.089

Figure 5-1. Standard Rating - SR-114 Stringers

Strength Limit State Rating Factors					
Model	Load	End Span M^+ RF	Interior Span M^+ RF	End Span M^- RF	Interior Span M^- RF
2-Span	HL-93 Inventory	1.306	NA	1.151	NA
3-Span	HL-93 Inventory	1.284	1.785	1.334	1.334
2-Span	HL-93 Operating	1.693	NA	1.493	NA
3-Span	HL-93 Operating	1.664	2.313	1.730	1.730
2-Span	Type 3 Legal	2.625	NA	2.991	NA
3-Span	Type 3 Legal	2.601	3.580	3.209	3.209
2-Span	Type 3S2 Legal	2.805	NA	2.431	NA
3-Span	Type 3S2 Legal	2.778	3.808	2.773	2.773
2-Span	Type 3-3 Legal	3.189	NA	3.105	NA
3-Span	Type 3-3 Legal	3.086	4.347	3.408	3.408
2-Span	Type NRL Legal	1.923	NA	2.423	NA
3-Span	Type NRL Legal	1.910	2.663	2.483	2.483

		Service Limit State Rating Factors		
Model	Load	Positive M_u	RF	RF
2-Span	HL-93 Inventory	496.0	1.195	1.027
3-Span	HL-93 Inventory	501.6	1.170	1.205
2-Span	HL-93 Operating	394.9	1.553	1.335
3-Span	HL-93 Operating	401.2	1.521	1.567
2-Span	Type 3 Legal	320.9	1.990	2.211
3-Span	Type 3 Legal	325.6	1.964	2.401
2-Span	Type 3S2 Legal	304.0	2.126	1.797
3-Span	Type 3S2 Legal	309.1	2.097	2.076
2-Span	Type 3-3 Legal	274.4	2.417	2.295
3-Span	Type 3-3 Legal	284.9	2.329	2.551
2-Span	Type NRL Legal	416.9	1.458	1.791
3-Span	Type NRL Legal	419.6	1.442	1.858

Fatigue Limit State Rating Factors		
2-Span	Fatigue	1.764
3-Span	Fatigue	1.828

Figure 5-2. Refined Rating - SR-114 Stringers

Chapter 6 Conclusion

Upon evaluation of the diagnostic load testing results, it can be inferred that the stringers in the girder-stringer-floorbeam bridge, SR-114 over the Tennessee River, have higher load ratings than initially anticipated. This is due, in part, to the fact that the stringers act semi-compositely with the concrete bridge deck (proven by the strain profile at the member cross-sections), which allows for a higher capacity in the stringers. In addition, the live load demands on the stringers were observed to be less than anticipated. Note that the primary refinements recommended in this report still consider the stringers to act non-compositely since extrapolation from load test levels to design levels is not appropriate.

A supplementary Excel spreadsheet was made that allows the user to determine the load rating for steel stringers using the "default" settings or using the modifiers that were discussed in Chapter 4. The modifiers that can be selected include the F_{cr} modifier, an envelope factor which accounts for a 15% increase in C_b if calculated based on moment envelopes rather than concurrent moments, Appendix A6 criteria, and a refined C_b. These modifiers provide substantial increases in the load ratings for stringers in SR-114 over the Tennessee River.

References

AASHTO. (2019). The Manual for Bridge Evaluation. Third Edition. American Association of State Highway and Transportation Officials. Washington, D.C.

AASHTO. (2020). AASHTO LRFD Bridge Design Specifications, Ninth Edition. American Association of State Highway and Transportation Officials. Washington, D.C.

AISC. (2017). ANSI/AISC 360-16: Specification for Structural Steel Building, Fifteenth Edition. Chicago, IL.

Barker, M. G., Hertnagel, B. A., Schilling, C. G. & Dishongh, B. E., (2000). Simplified Inelastic Design of Steel Girder Bridges. ASCE Journal of Bridge Engineering, 9(3), 230-242.

Barth, K. E., Hartnagel, B. A., White, D. W. & Barker, M. G., (2004). Recommended Procedures for Simplified Inelastic Design of Steel I-Girder Bridges. ASCE Journal of Bridge Engineering, 9(3), 230-242.

Barth, K. E. & W., W. D., (2000). Inelastic Design of Steel I-Girder Bridges. ASCE Journal of Bridge Engineering, 179-190.

Breña, S. F., Jeffrey, A. E., & Civjan, S. A. (2013). Evaluation of a noncomposite steel girder bridge through live-load field testing. ASCE Journal of Bridge Engineering, 18 (7), 690-699.

Don, D. M. K. K. A., (2021). Lateral Torsional Buckling Resistance of Continuous Steel Stringers in Existing Bridges, Ruston LA: Louisiana Tech University College of Engineering and Science.

FHWA, (2015). Steel Bridge Design Handbook. Federal Highway Administration. Washington, D.C.

Ghosn, M. & Moses, F., (1998). NCHRP Report 406: Redundancy in Highway Bridge Superstructures. Transportation Research Board - National Cooperative Highway Research Program. Washington, D.C.

Kuruppuarachchi, K. A. D. D. M., (2021). Lateral Torsional Buckling Resistance of Continuous Steel Stringers in Existing Bridges, Baton Rouge: College of Engineering and Science, Louisiana Tech University.

McConnell, J. R. & Barth, K., (2010). Rotation Requirements for Moment Redistribution in Steel Bridge I-Girders. ASCE Journal of Bridge Engineering, 15(3), 279-289.

Nethercot, D. A. & Rocky, K. C., (1972). A Unified Approach to the Elastic Lateral Buckling of Beams. AISC Engineering Journal, 9(3), 96-107.

Schilling, C. G., (1998). Simplified Inelastic Design of Steel Girder Bridges. Engineering Journal, 147-158.

Sun, C. S., Linzell, D. G. & Puckett, J. A., (2021). Load Rating of Existing Continuous Stringers on Louisiana's Bridges, Baton Rouge: Civil Engineering Program, Louisiana Tech University.

Taylor, A. C., (1964). Torsional Restraint of Lateral Buckling - PhD Dissertation, Columbus: Ohio State University.

Tomlinson, S., Davids, W., Albraheemi, M., & Schanck, A. (2016). Instrumentation During Live Load Testing and Load Rating of Five Slab-On-Girder Bridges (No. ME 18-2).

Valentino, A. & Trahair, N. S., (1998). Torsional Restraint Against Elastic Lateral Buckling. ASCE Journal of Structural Engineering, 124(10), 1217-1225.

Yura, J. A., (2001). Fundamentals of Beam Bracing. AISC Engineering Journal, Volume 38, 11-26.

Yura, J. A. & Helwig, T. A., (2010). Buckling of Beams with Inflection Points. s.l., Structural Stability Research Council, 761-780.